Low Complexity Generic Receiver for the NATO Narrow Band Waveform

Vincent Le Nir and Bart Scheers
Department Communication, Information, Systems & Sensors (CISS)
Royal Military Academy
Brussels, BELGIUM
Email: {vincent.lenir,bart.scheers}@rma.ac.be

***Abstract*—The principal objective of the NATO Narrow Band Waveform (NBWF) is to achieve coalition interoperability within lower tactical levels. This paper describes a low-complexity generic receiver for the different modes of the NBWF. The NBWF burst consists of a continuous wave (CW) signal followed by a pseudo-random sequence and a data sequence modulated by continuous phase modulation (CPM). Joint coarse carrier frequency, phase and time synchronization is performed on the CW signal. Fine time synchronization is performed on the CW and CPM pseudo-random sequence signals. Fine carrier frequency and phase synchronization is performed on the full burst. The main idea is to transform the CPM signal with modulation index $h < 1/2$ into a CPM signal with modulation index $h = 1/2$ by exponentiation so that the signal can be demodulated with a generic linear demodulator based on Laurent's filters. Simulations are conducted to evaluate the performance of the different NBWF modes and the different algorithms. Simulation results confirm that the low complexity receiver achieves good performance and can be applied on all NBWF modes.**

I. Introduction

There is currently no narrowband Combat Net Radio (CNR) STANAG waveform for international and combined missions providing interoperability in Network Centric Operations (NCO). The principal objective of the Narrow Band Waveform (NBWF) is to achieve coalition interoperability within lower tactical levels [1].

The NBWF uses bandwidths of 25 KHz and 50 kHz with on-air bit rates up to 82 kbps in the very high frequency (VHF) or lower ultra high frequency (UHF) bands with continuous phase modulation (CPM). CPM has the advantages of high spectral efficiency due to the phase continuity and high power efficiency due to the constant envelope. However, CPM has the disadvantage of the high implementation complexity required to build an optimal receiver [2]. CPM has been used in several well-known communications protocols such as GSM and Bluetooth.

Comparing with similar works about NBWF receiver implementations [3], [4], [5], this paper describes a low-complexity generic receiver for the different modes of the NBWF. An innovative approach concerning coarse and fine frequency, phase and time synchronizations and demodulation is presented. This approach minimizes and simplifies the receiver, which is important in military portable equipment.

The NBWF burst consists of a continuous wave (CW) signal followed by a pseudo-random sequence and a data sequence modulated by CPM. The low-complexity generic receiver can be split into the following tasks :

- Joint coarse carrier frequency, phase and time synchronization is performed on the CW signal. The synchronization algorithm is an extension of the iterative frequency estimation algorithm by interpolation on Fourier coefficients described in [6] to take into account carrier phase and time synchronization. The synchronization algorithm searches for the time offset whose estimated iterative frequency offset has the maximum power and determines the phase offset of the CW signal at the time and frequency offset estimates.
- Fine time synchronization is performed on the CW and CPM pseudo-random sequence signals similarly to [4]. A peak search of the correlation function between the received signal and a stored CW and CPM pseudo-random sequence around the estimated coarse time offset is performed.
- Due to errors in the joint coarse carrier frequency, phase and time synchronization on the CW signal, fine carrier frequency and phase synchronization is performed on the full burst taking into account fine time synchronization. Two fine carrier frequency and phase synchronization algorithms are studied in this paper. The first algorithm is a data aided (DA) carrier frequency and phase synchronization algorithm applied to the CW and CPM pseudo-random sequence signals. The second algorithm is a non data aided (NDA) carrier frequency and phase synchronization algorithm applied to the full burst. The second algorithm is an extension of the NDA feed forward carrier frequency synchronization algorithm with minimum shift keying (MSK)-type signals as described in [7]. The extended algorithm downsamples the signal at the symbol rate, transforms the resulting signal into a CPM signal with four constellation points, takes the fourth power of the transformed signal, and applies the iterative frequency estimation algorithm [6] on the fourth powered signal at the time offset estimate.
- For a constant symbol rate in CPM, lower modulation indexes ($h < 1/2$) in combination with partial response CPM with inter symbol interference (ISI) ($L > 1$) narrows the spectrum. The different NBWF modes use

constant bandwidths of 25 KHz and 50 kHz with lower modulation indexes ($h < 1/2$) in combination with partial response CPM with ISI ($L > 1$) to achieve higher symbol rates. Exponentiation transforms the CPM signal with modulation index $h < 1/2$ into a CPM signal with modulation index $h = 1/2$. An implementation of the transformation of a CPM signal with small modulation index into a CPM signal with modulation index $h = 1/2$ is described in [8].

- Linear demodulation filters the synchronized signal with the first pulse of Laurent's linear representation of CPM signals [9], [10]. The linear demodulator has the advantage of a good trade off between performance and complexity compared to maximum-likelihood receivers implemented using Viterbi or iterative algorithms [3], [5], [11], [12].
- Decision logic is applied to the filtered signal to recover the data sequence. As the Laurent's linear representation of CPM signals with modulation index $h = 1/2$ transforms the information symbols belonging to the binary alphabet $\{\pm 1\}$ into differential encoded symbols, the decision logic algorithm performs a modified version of the differential decoder [10] using the real and imaginary received samples to reduce ISI.

The paper is organized as follows. In section II, we present the signal model. More specifically, the complex baseband representation of a CPM signal and the burst-mode transmission model of the NBWF are presented. In section III, the different algorithms of the low-complexity receiver are described. These are the joint coarse carrier frequency, phase and time synchronization algorithm, the fine time synchronization algorithm, the fine carrier frequency and phase synchronization algorithm, the exponentiation algorithm, the linear demodulation algorithm and the decision logic algorithm. In Section IV, simulations are conducted to show the influence of the different NBWF modes on the different algorithms. Finally, section V concludes the paper.

II. Signal Model

A. Representation of a CPM signal

The complex baseband representation of a CPM signal is given by

$$x(t, \mathbf{a}) = e^{j\psi(t,\mathbf{a})} \tag{1}$$

$$\psi(t, \mathbf{a}) = \pi h \sum_i a_i q(t - iT) \tag{2}$$

with h the modulation index, T the symbol period, $\mathbf{a} = \{a_i\}$ the information belonging to the binary alphabet $\{\pm 1\}$, $q(t)$ the phase response of the system with $q(t) = \int_0^t g(u)du$ and satisfying the condition $q(LT) = 1$, L the pulse length, $g(t)$ the shaping pulse time-limited to the interval $[0, LT]$ and satisfying the condition $g(t) = g(LT - t)$. Full response CPM corresponds to $L = 1$. Partial response CPM corresponds to $L > 1$. MSK-type modulation corresponds to a binary CPM with $h = 1/2$. The most important shaping pulses are the rectangular (LREC), raised-cosine (LRC), spectral raised cosine (LSRC), Gaussian and tamed FM as defined in [2]. The NBWF uses the rectangular shaping pulse with pulse length $L = 2, 3$ and modulation index $h = 1/2, 1/4, 1/6, 1/9$ [1].

B. Laurent's representation of a CPM signal

Laurent [9] showed that the complex baseband representation of a CPM signal (1) can be written as a sum of $K = 2^{L-1}$ pulse amplitude modulation (PAM) signals

$$x(t, \mathbf{a}) = \sum_i \sum_{k=0}^{K-1} b_{k,i} c_k(t - iT) \tag{3}$$

with $b_{k,i}$ a function of the information sequence $\{a_i\}$ and $c_k(t)$ an equivalent shaping pulse of the k^{th} PAM signal [10]. Laurent also showed that $c_0(t)$, which represents the pulse of longest duration $(L + 1)T$, also happens to have the highest energy and is the most important component of the signal [9]. Therefore, the baseband signal (1) can be approximated as

$$x(t, \mathbf{a}) \approx \sum_i b_{0,i} c_0(t - iT) \tag{4}$$

$$b_{0,i} = b_{0,i-1} e^{j\pi h a_i} \tag{5}$$

$$c_0(t) = \prod_{l=0}^{L-1} p(t + lT) \tag{6}$$

$$p(t) = \begin{cases} \dfrac{\sin(\pi h q(t))}{\sin(\pi h)} & 0 \le t \le LT \\ \dfrac{\sin(\pi h (1 - q(t - LT)))}{\sin(\pi h)} & LT \le t \le 2LT \\ 0 & \text{otherwise} \end{cases} \tag{7}$$

Assuming transmission over an additive white Gaussian noise (AWGN) channel, the complex baseband representation of the received signal can be written as

$$\begin{aligned} y(t, \mathbf{a}) &= A e^{j(2\pi\alpha t + \phi)} x(t - \tau, \mathbf{a}) + n(t) \\ &\approx A \sum_i b_{0,i-1} e^{j(\pi h a_i + 2\pi\alpha t + \phi)} c_0(t - \tau - iT) + n(t) \end{aligned} \tag{8}$$

with A the received signal amplitude, α the carrier frequency offset, ϕ the carrier phase offset, τ the time offset and $n(t)$ the AWGN with variance $N_0/2$ per dimension. The received samples can be written as

$$y(k) = y(t, \mathbf{a}) \Big|_{t = \frac{kT}{F}} \tag{9}$$

with F the oversampling factor.

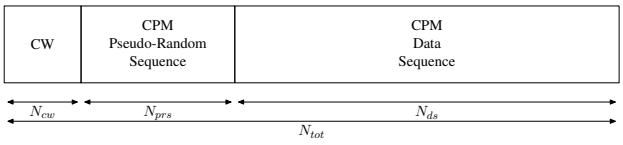

Fig. 1. Structure of the burst

C. Burst-mode transmission model of the NBWF

The burst-mode transmission model of the NBWF considers the transmission of independent bursts. Each burst has a known duration and structure as described in [4] and shown in Figure 1.

The burst of length N_{tot} consists of a CW signal of length N_{cw}, a CPM pseudo-random sequence signal of length N_{prs} and a CPM data sequence signal of length N_{ds}. Such burst structure has already been adopted in [4], in which the authors exploit the CW signal for carrier frequency and phase synchronization and the CPM pseudo-random sequence signal for time synchronization. However, exploiting only the CW signal for carrier frequency and phase synchronization leads to a low accuracy of the carrier frequency and phase estimates for the different modes of the NBWF. In this paper, two fine carrier frequency and phase synchronization algorithms are studied. The first algorithm is a DA carrier frequency and phase synchronization algorithm applied to the CW and CPM pseudo-random sequence signals. The second algorithm is a NDA carrier frequency and phase synchronization algorithm applied to the full burst. These algorithms allow to obtain a higher accuracy of the carrier frequency and phase estimates for the different modes of the NBWF.

III. Low-Complexity Receiver

The low-complexity generic receiver depicted in Figure 2 is described in the following paragraphs.

A. Joint coarse carrier frequency, phase and time synchronization

Joint coarse carrier frequency, phase and time synchronization is performed on the CW signal. The synchronization algorithm is an extension of the iterative frequency estimation algorithm by interpolation on Fourier coefficients described in [6] to take into account carrier phase and time synchronization. Let N_{cw} the number of samples of the CW signal, N_{tot} the total number of samples of the burst, $\hat{\alpha}$ the estimated carrier frequency offset with $\hat{\beta}$ the integer part of the estimated carrier frequency offset and $\hat{\delta}$ the non-integer part of the estimated frequency offset. The extended algorithm is described in Algorithm 1 with $N = N_{cw}$.

Algorithm 1 Joint coarse carrier frequency, phase and time synchronization algorithm

Loop : for all k, $y_k = [y(k) \dots y(k+N)]$
  Let $Y_k = FFT(y_k)$, $E_k(i) = |Y_k(i)|^2$, $i = 0 \dots N-1$
  Find $\hat{\beta} = \underset{i}{argmax}\ \ E_k(i)$
  Set $\hat{\delta}_0 = 0$
  Loop : for each i from 1 to Q
    $X_p = \sum_{n=0}^{N-1} y(n) e^{-j2\pi n \frac{\hat{\beta}+\hat{\delta}_{i-1}+p}{N}}, p = \pm 0.5$
    $\hat{\delta}_i = \hat{\delta}_{i-1} + \frac{1}{2} Re\left\{ \frac{X_{0.5}+X_{-0.5}}{X_{0.5}-X_{-0.5}} \right\}$
  $X_{0,k} = \sum_{n=0}^{N-1} y(n) e^{-j2\pi n \frac{\hat{\beta}+\hat{\delta}_Q}{N}}$
  $\hat{\alpha}_k = \frac{\hat{\beta}+\hat{\delta}_Q}{N}$
Coarse time offset estimate : $\hat{\tau} = \underset{k}{argmax} |X_{0,k}|^2$
Coarse carrier frequency offset estimate : $\hat{\alpha} = \alpha_{\hat{\tau}}$
Coarse carrier phase offset estimate : $\hat{\phi} = arg(X_{0,\hat{\tau}})$

This algorithm searches for the time offset whose estimated iterative frequency offset has the maximum power. The carrier frequency offset estimate is the carrier frequency offset at the time offset estimate. The carrier phase offset estimate is the carrier phase offset of the CW signal at the time and frequency offset estimates.

B. Fine time synchronization

Fine time synchronization is performed on the addition of the CW signal and the CPM pseudo-random sequence signal. A peak search of the correlation function between the received signal and a stored CW signal plus CPM pseudo-random sequence signal around the estimated coarse time offset is performed. Assuming $N = N_{cw} + N_{prs}$, the optimization problem can be written as

$$\hat{\tau} = \underset{k}{argmax}\ \ |r(k)|^2 \tag{10}$$

with

$$r(k) = \frac{1}{N} \sum_{n=0}^{N-1} y(n+k) x^*(n) \quad k \in [\hat{\tau} - \frac{N_{cw}}{2} \dots \hat{\tau} + \frac{N_{cw}}{2}] \tag{11}$$

C. Fine carrier frequency and phase synchronization

Due to errors in the joint coarse carrier frequency, phase and time synchronization on the CW signal, fine carrier frequency and phase synchronization is performed on the full burst taking into account fine time synchronization. Two fine carrier frequency and phase synchronization algorithms are studied in this paper. The first algorithm is a DA carrier frequency and phase synchronization algorithm applied to the CW and CPM pseudo-random sequence signals. The second algorithm is a NDA carrier frequency and phase synchronization algorithm applied to the full burst.

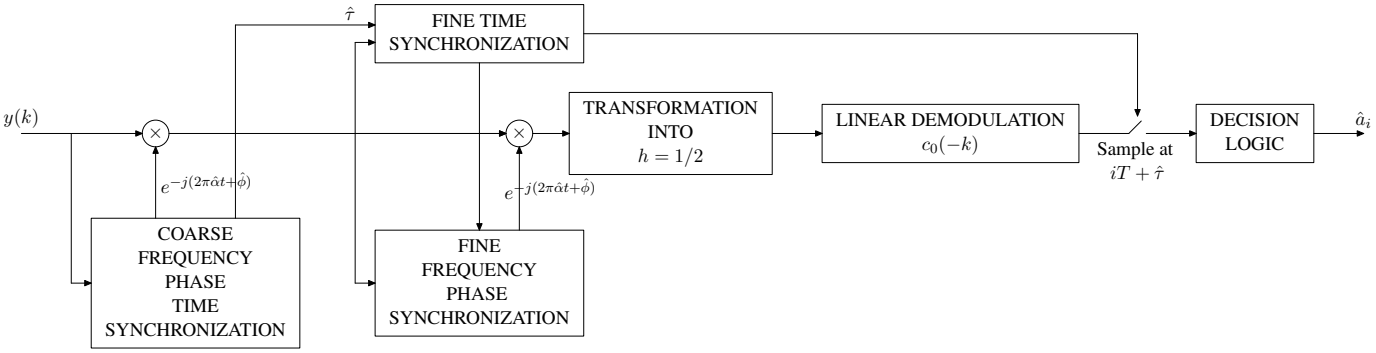

Fig. 2. Block diagram of the low-complexity receiver

1) Data aided fine carrier frequency and phase synchronization: This algorithm applies the iterative frequency estimation algorithm by interpolation on Fourier coefficients described in [6] to the correlation function between the received signal and a stored CPM pseudo-random sequence signal at the time offset estimate. The algorithm is described in Algorithm 2 with $N = N_{cw} + N_{prs}$ and $z = [z(0) \dots z(N-1)$ with

$$z(k) = y(k)x^*(k + \hat{\tau}) \tag{12}$$

Finally, the DA carrier frequency estimate is given by $\hat{\alpha} = \frac{\hat{\beta}+\hat{\delta}_Q}{N}$, and the DA carrier phase estimate by $\hat{\phi} = arg(X_0)$.

2) Non data aided fine carrier frequency and phase synchronization: The second algorithm is an extension of the NDA feed forward carrier frequency synchronization algorithm with MSK-type signals as described in [7]. We assume that the received signal is low-pass filtered to eliminate out-of-band noise and sampled at symbol rate $1/T$. The extended algorithm uses exponentiation to transform the CPM signal with modulation index $h < 1/2$ into a CPM signal with modulation index $h = 1/2$. An implementation of the transformation of a CPM signal with small modulation index into a CPM signal with modulation index $h = 1/2$ is described in [8]. Exponentiation can also be described by the following method

$$\tilde{\psi}(k) = \frac{arg(y(k))}{h}\frac{1}{2} \tag{13}$$

The received signal is then reconstructed by the following formula

$$\tilde{y}(k) = e^{j\tilde{\psi}(k)} \tag{14}$$

The reconstructed signal is a CPM signal with four constellation points for any shaping pulse whenever the pulse length $L = 1, 2$. For $L = 3$ with rectangular pulse, an additional exponentiation of 3rd power is necessary to obtain a CPM signal with four constellation points. In [7], a quadratic non linearity (QNL) is applied on the received signal $z(k) = (-1)^k\tilde{y}(k)^2$ for CPM signals without ISI or pulse length $L = 1$. However, this QNL does not apply for partial response CPM with ISI ($L > 1$). After the transformation of the received signal into a CPM signal with four constellation points by exponentiation, we propose to take the fourth power of the transformed signal $z(k) = \tilde{y}(i)^4$, and to apply the iterative frequency estimation algorithm [6] on the resulting signal. The algorithm can also be described in Algorithm 2 with $N = N_{cw} + N_{prs} + N_{ds}$ and $z = [z(0) \dots z(N-1)]$.

Algorithm 2 Iterative frequency estimation algorithm for DA and NDA carrier frequency and phase synchronization algorithms

Let $Z = FFT(z)$, $E(k) = |Z(k)|^2$, $k = 0 \dots N-1$
Find $\hat{\beta} = \underset{k}{argmax}\ \ E(k)$
Set $\hat{\delta}_0 = 0$
Loop : for each i from 1 to Q
    $X_p = \sum_{n=0}^{N-1} z(n)e^{-j2\pi n\frac{\hat{\beta}+\hat{\delta}_{i-1}+p}{N}}, p = \pm 0.5$
    $\hat{\delta}_i = \hat{\delta}_{i-1} + \frac{1}{2}Re\left\{\frac{X_{0.5}+X_{-0.5}}{X_{0.5}-X_{-0.5}}\right\}$
$X_0 = \sum_{n=0}^{N-1} z(n)e^{-j2\pi n\frac{\hat{\beta}+\hat{\delta}_Q}{N}}$

Finally, the NDA carrier frequency estimate is given by $\hat{\alpha} = \frac{\hat{\beta}+\hat{\delta}_Q}{N}\frac{h}{4}$, and the NDA carrier phase estimate by $\hat{\phi} = arg(X_0)\frac{h}{4}$ for $L = 2$. For $L = 3$, a further exponentiation of 3rd power is applied on equation (13) and a division by three is necessary on the NDA carrier frequency and phase estimates.

D. Transformation into a CPM signal with $h = 1/2$

The CPM signal with modulation index $h < 1/2$ is transformed into a CPM signal with modulation index $h = 1/2$ with four constellation points while keeping the initial phase offset. The transformation is described by the following method

$$\tilde{\psi}(k) = \frac{arg(y(k))}{h}\frac{1}{2} + (\frac{1}{h} - 2)\frac{\pi}{8} \tag{15}$$

for even $1/h$ numbers. For odd $1/h$ numbers, an additional phase unwrapping is necessary

Algorithm 3 Phase unwrapping for odd $1/h$ numbers

```
Loop : for all k
    if ψ̃(k) − ψ̃(k − 1) > 2π
        ψ̃(k) = ψ̃(k) − π
    if ψ̃(k) − ψ̃(k − 1) < 2π
        ψ̃(k) = ψ̃(k) + π
```

The received signal is then reconstructed by the following formula

$$\tilde{y}(k) = e^{j\tilde{\psi}(k)} \tag{16}$$

Similarly to the NDA fine carrier frequency and phase synchronization algorithm, the reconstructed signal is a CPM signal with four constellation points for any shaping pulse whenever the pulse length $L = 1, 2$. For $L = 3$, an additional exponentiation of 3rd power is necessary to obtain a CPM signal with four constellation points.

E. Linear demodulation

Linear demodulation filters the synchronized signal with the first pulse of Laurent's linear representation of CPM signals. The linear demodulator has the advantage of a good trade off between performance and complexity compared to maximum-likelihood receivers implemented using Viterbi or iterative algorithms [3], [5], [11], [12]. The convolution and sampling operation can be written as

$$s(i) = (y * c_0)(k)\,|_{k=Fi+\hat{\tau}} \tag{17}$$

F. Decision Logic

Decision logic is applied to the filtered signal to recover the data sequence. As the Laurent's linear representation of CPM signals with modulation index $h = 1/2$ transforms the information symbols belonging to the binary alphabet $\{\pm 1\}$ into differential encoded symbols, the decision logic algorithm performs a modified version of the differential decoder [10] using the real and imaginary received samples to reduce ISI.

$$\hat{a}_i = \begin{cases} \text{Im}(s(i))\text{Re}(s(i-1)) & i \text{ even} \\ -\text{Re}(s(i))\text{Im}(s(i-1)) & i \text{ odd} \end{cases} \tag{18}$$

IV. Simulation Results

Simulations are conducted to evaluate the performance of the different NBWF modes and the different algorithms. Figure 3 shows the mean square error (MSE) performance vs signal to noise ratio (SNR) of the different carrier frequency and phase synchronization algorithms with the different NBWF modes shown in Table I. The CW carrier and phase synchronization algorithm is applied to the CW signal of length N_{cw}. The DA carrier frequency and phase synchronization algorithm is applied to the CW and CPM pseudo-random sequence signals of length $N_{cw} + N_{prs}$. The NDA carrier frequency and phase synchronization algorithm is applied on the full burst $N_{cw} + N_{prs} + N_{ds}$. The Cramer-Rao bounds of the different NBWF modes are given for reference and are given by [13]

TABLE I
NBWF Modes

Mode	Data Rate (kbps)	h	Pulse Shape	Code Rate	Symbol Rate (ksps)	BW (kHz)
NR	10	1/2	2-REC	1/3	30	25
N1	20	1/2	2-REC	2/3	30	25
N2	31.5	1/4	2-REC	3/4	42	25
N3	64	1/6	3-REC	4/5	80	25
N4	82	1/9	3-REC	6/7	96	25
N5	40	1/2	2-REC	2/3	60	50
N6	63	1/4	2-REC	3/4	84	50

$$CRB = \frac{6}{N(N^2-1)}\frac{1}{SNR} \tag{19}$$

with N the number of samples and SNR the signal to noise ratio. A total of 10^4 Monte Carlo trials are used to generate the simulation results with carrier frequency offsets in the range $\alpha \in]-0.25h, 0.25h[$ for $L = 2$ and $\alpha \in]-0.25h/L, 0.25h/L[$ for $L = 3$. Figure 3 shows that the CW and DA carrier frequency and phase synchronization algorithms reaches the CRB at the SNR threshold SNR=0 dB and SNR=-4 dB respectively, for any modulation index and any pulse length L. As the DA carrier frequency and phase synchronization algorithm is applied on a larger number of samples, its CRB is lower than the CW carrier frequency and phase synchronization algorithm. Therefore, exploiting only the CW signal for carrier frequency and phase synchronization leads to a low accuracy of the carrier frequency and phase estimates for the different modes of the NBWF. As the NDA carrier frequency and phase synchronization algorithm is applied on the full burst, its CRB is lower than the DA carrier frequency and phase synchronization algorithm. The SNR threshold value of the NDA carrier frequency and phase synchronization algorithm increases as the modulation index decreases and as the pulse length increases, SNR=5-6 dB for mode NR, N1, N5 with $h = 1/2, L = 2$, SNR=11 dB for mode N2, N6 with $h = 1/4, L = 2$, SNR=24 dB for mode N3 with $h = 1/6, L = 3$, and SNR=28 dB for mode N4 with $h = 1/9, L = 3$. For SNRs higher than the threshold, the MSE performance of the NDA carrier frequency and phase synchronization algorithm is better than the CW and DA carrier frequency and phase synchronization algorithms because of the lower CRB.

Figure 4 shows the BER performance vs SNR of the low-complexity generic receiver with the different NBWF modes shown in Table I. The genie aided (GA) BER curves correspond to the case of perfect carrier frequency and phase estimates. The GA BER curves are the theoretical references to compare with the different algorithms. The DA BER curves corresponds to the DA fine carrier frequency and phase synchronization algorithm. The NDA BER curves corresponds to the NDA fine carrier frequency and phase synchronization algorithm. Figure 4 shows that the BER performance decreases as the modulation index h decreases and as the pulse length L increases. This is a direct consequence of the linear approximation. Moreover, it can be observed that the NDA fine

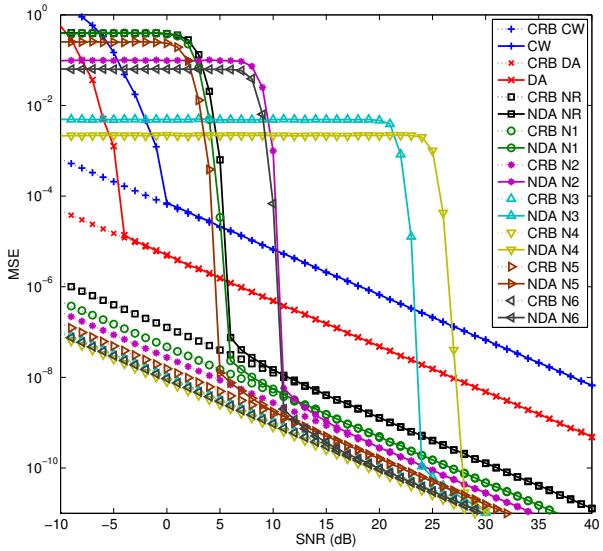

Fig. 3. MSE performance of the different algorithms for all NBWF modes

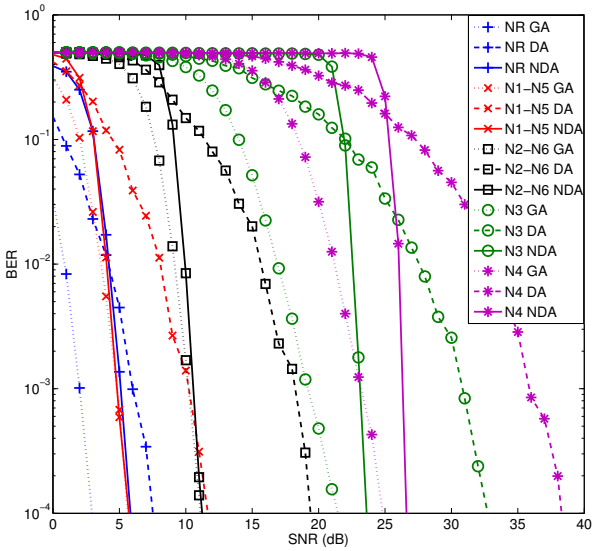

Fig. 4. BER performance of the different algorithms for all NBWF modes

carrier frequency and phase synchronization algorithm has better performance than the DA fine carrier frequency and phase synchronization algorithm for all NBWF modes. The performance of the NDA fine carrier frequency and phase synchronization algorithm is close to the performance of GA for low BERs and modes N1, N2, N5, and N6. This is due to the structure of the NBWF bursts [1] which have less DA than NDA symbols $N_{cw} < N_{prs} < N_{ds}$. For higher BERs and other modes (NR, N3, N4), there is still a gap between the performance of GA and the DA or NDA fine carrier frequency and phase synchronization algorithms, meaning that there is still room for improved synchronization algorithms.

The low-complexity generic receiver for the different modes of the NBWF has been successfully implemented in C++ using open-source libraries (Qt, UHD, IT++, GStreamer) and tested on Odroid-XU4 single board computers attached with a USRP B205-mini software defined radios. The NBWF physical and data link layers [1], [14] are able to run in real-time on these general purpose processors (GPP) owing to the low-complexity generic receiver, this would have not been possible with maximum-likelihood receivers implemented using Viterbi or iterative algorithms [3], [5], [11], [12].

V. Conclusion

This paper has described a low-complexity generic receiver for the different NBWF modes. The NBWF burst consists of a continuous wave (CW) signal followed by a pseudo-random sequence and a data sequence modulated by continuous phase modulation (CPM). Joint coarse carrier frequency, phase and time synchronization is performed on the CW signal. Fine time synchronization is performed on the CPM pseudo-random sequence signal. Fine carrier frequency and phase synchronization is performed on the CPM signal. Exponentiation transforms the CPM signal with modulation index $h < 1/2$ into a CPM signal with modulation index $h = 1/2$. Linear demodulation filters the synchronized signal with the first pulse of Laurent's linear representation of CPM signals. Decision logic is applied to the filtered signal to recover the data sequence. Simulations were conducted to evaluate the performance of the different NBWF modes and the different algorithms. Simulations have shown that exploiting only the CW signal for carrier frequency and phase synchronization leads to a low accuracy of the carrier frequency and phase estimates for the different modes of the NBWF. Moreover, it has been observed that the NDA fine carrier frequency and phase synchronization algorithm has better performance than the DA fine carrier frequency and phase synchronization algorithm for all NBWF modes. The performance of the NDA fine carrier frequency and phase synchronization algorithm is close to the performance of GA for low BERs and modes N1, N2, N5, and N6. This is due to the structure of the NBWF bursts which have less DA than NDA symbols $N_{cw} < N_{prs} < N_{ds}$. For higher BERs and other modes (NR, N3, N4), there is still a gap between the performance of GA and the DA or NDA fine carrier frequency and phase synchronization algorithms, meaning that there is still room for improved synchronization algorithms. The low-complexity generic receiver for the different modes of the NBWF has been successfully implemented in C++ using open-source libraries (Qt, UHD, IT++, GStreamer) and tested on Odroid-XU4 single board computers attached with a USRP B205-mini software defined radios. The NBWF physical and data link layers are able to run in real-time on these general purpose processors (GPP) owing to the low-complexity generic receiver, this would have not been possible

with maximum-likelihood receivers implemented using Viterbi or iterative algorithms.

REFERENCES

[1] *Narrowband Waveform for VHF/UHF Radio - Physical Layer Standard and Propagation Models*, STANAG 5631/AComP-5631, Edition 1.0 Ratification Draft, NATO Unclassified, January 2015.

[2] J. Anderson, T. Aulin and C. Sundberg, *Digital Phase Modulation*, New York: Plenum, 1986.

[3] C. Brown and P. Vigneron, *Coarse and Fine Timing Synchronization for Partial Response CPM in a Frequency Hopped Tactical Network*, IEEE Conference on Military Communications, Orlando, USA, October 2007.

[4] J. Pugh, C. Brown and P. Vigneron, *Preamble design and acquisition for CPM*, Proc. SPIE 7706, Wireless Sensing, Localization, and Processing V, April 2010.

[5] E. Casini, D. Fertonani and G. Colavolpe, *Advanced CPM receiver for the NATO tactical narrowband waveform*, IEEE Conference on Military Communications, San Jose, USA, December 2010.

[6] E. Aboutanios and B. Mulgrew, *Iterative Frequency Estimation by Interpolation on Fourier Coefficients*, IEEE Transactions on Signal Processing, Vol. 53 , No. 4, April 2005.

[7] M. Morelli and U. Mengali, *Feedforward Carrier Frequency Estimation with MSK-Type Signals*, IEEE Communications Letters, Vol. 2, No. 8, August 1998.

[8] Z. Xi, J. Zhu and Y. Fu, *Low-Complexity Detection of Binary CPM With Small Modulation Index*, IEEE Communications Letters, Vol. 20, No. 1, January 2016.

[9] P. Laurent, *Exact and approximate construction of digital phase modulations by superposition of amplitude modulated pulses (AMP)*, IEEE Transactions on Communications, Vol. COM-34, pp. 150-160, February 1986.

[10] G. Kaleh, *Simple Coherent Receivers for Partial Response Continuous Phase Modulation*, IEEE Journal on Selected Areas in Communications, Vol. 7, No.9, pp. 1427-1436, December 1989.

[11] G. Lui and K. Tsai, *Viterbi and serial demodulators for pre-coded binary GMSK*, International Telemetering Conference, Las Vegas, Nevada, October 1999.

[12] A. Barbieri and G. Colavolpe, *Simplified Soft-Output Detection of CPM Signals Over Coherent and Phase Noise Channels*, IEEE Transactions on Wireless Communications, Vol. 6, No. 7, July 2007.

[13] S. Kay, *A fast and accurate single frequency estimator*, IEEE Transactions on Acoustics, Speech, Signal Processing, 1989, **37**, pp. 1987-1990.

[14] *Narrowband Waveform for VHF/UHF Radio - Link Layer Standard*, STANAG 5632/AComP-5632, Edition 1.0 Ratification Draft, NATO Unclassified, January 2015.